(2)

1. AGENC

September 8,1993 Reprint

3. REPORT TYPE AND DATES COVERED

4. TITLE AND SUBTITLE

Comment on the Transmission-Line Model for Computing Radiation From Lightning

5. FUNDING NUMBERS

PE 62101F
PR 6670
TA GX
WU 12

6. AUTHOR(S)

D.M. Le Vine*, J.C. Willett

7. PERFORMING ORGANIZATION NAME(S) AND ADDRESS(ES)

Phillips Lab/GPAA
29 Randolph Road
Hanscom AFB, MA 01731-3010

8. PERFORMING ORGANIZATION REPORT NUMBER

PL-TR-93-2188

*Microwave Sensors Branch, Goddard Space Flight Center, Greenbelt, Maryland

Reprinted from Journal of Geophysical Research, Vol. 97, No. D2, pages 2601-2610
February 20, 1992

Approved for public release; Distribution unlimited

The "transmission-line" model is an approximation that is frequently used to relate the electric and magnetic fields radiated during lightning discharges to the currents that produce those fields. A principal prediction of this model is that the distant (radiation) fields are directly proportional to the current propagating along the lightning channel, multiplied by the velocity of propagation. This paper examines the derivation of this relationship and its implications in some detail. We show that the formulas commonly used to describe the transmission-line model cannot be correctly applied to many lightning processes. A correction factor is required that is significant when the channel is not oriented perpendicular to the line of sight to the observer, unless the propagation velocity is only a small fraction of the speed of light. An important implication of this more general version of the model is that the current and velocity decouple so that they could be separately determined by suitable, multistation measurements.

14. SUBJECT TERMS

Lightning; Return Stroke; Radiation Field; Transmission-Line Model

15. NUMBER OF PAGES

10

16. PRICE CODE

17. SECURITY CLASSIFICATION OF REPORT	18. SECURITY CLASSIFICATION OF THIS PAGE	19. SECURITY CLASSIFICATION OF ABSTRACT	20. LIMITATION OF ABSTRACT
UNCLASSIFIED	UNCLASSIFIED	UNCLASSIFIED	SAR

PL-TR-93-2188

JOURNAL OF GEOPHYSICAL RESEARCH, VOL. 97, NO. D2, PAGES 2601-2610, FEBRUARY 20, 1992

Comment on the Transmission-Line Model for Computing Radiation From Lightning

D. M. LE VINE

Microwave Sensors Branch, Goddard Space Flight Center, Greenbelt, Maryland

J. C. WILLETT

Geophysics Directorate, Phillips Laboratory, Hanscom Air Force Base, Massachusetts

The "transmission-line" model is an approximation that is frequently used to relate the electric and magnetic fields radiated during lightning discharges to the currents that produce those fields. A principal prediction of this model is that the distant (radiation) fields are directly proportional to the current propagating along the lightning channel, multiplied by the velocity of propagation. This paper examines the derivation of this relationship and its implications in some detail. We show that the formulas commonly used to describe the transmission-line model cannot be correctly applied to many lightning processes. A correction factor is required that is significant when the channel is not oriented perpendicular to the line of sight to the observer, unless the propagation velocity is only a small fraction of the speed of light. An important implication of this more general version of the model is that the current and velocity decouple so that they could be separately determined by suitable, multistation measurements.

1. INTRODUCTION

In the "transmission-line" model for lightning discharges it is assumed that the current propagates along the channel at constant velocity and without changing shape. That is, it is assumed that the current advances up the channel as a traveling wave, $i(\vec{r}', t) = I(t - \hat{l} \cdot \vec{r}'/v)$, where v is the velocity of propagation, $\hat{l}$ is a unit vector in the direction of the propagation along the channel (assumed to be straight), and $\vec{r}'$ is the position vector of a point on the channel. That current should propagate along the channel was originally suggested by *Dennis and Pierce* [1964] as a means of addressing physical inconsistencies in the Bruce-Golde model [*Bruce and Golde*, 1941], and this concept was developed in detail by Uman and colleagues [*Uman and McLain*, 1969, 1970; *McLain and Uman*, 1971; *Uman et al.*, 1975*a*, *b*; *Lin et al.*, 1980; and others].

The term transmission-line model is attributable to *Uman and McLain* [1969, 1970], who also were the first to show that when the observation point is far from the channel the transmission-line model indicates that the radiated magnetic field is proportional to the current waveform, $I(t)$, propagating up the channel [*Uman and McLain*, 1970]. The formula obtained by *Uman and McLain* [1970, equations (11) and (12)] provides a means of determining the current remotely from measurements of the radiated magnetic field and an assumed value of the propagation velocity. The equivalent formula for the electric field was applied recently to return strokes in triggered lightning, in experiments in which current, electric field, and velocity all were measured, to test the model [*Willett et al.*, 1988, 1989].

An appealing attribute of the transmission-line model is that it yields a simple, analytic formula relating channel current to radiation field. The version of the model described above, however, applies only to a straight, vertical channel and to an observer on the ground far from the channel base. The current waveform and propagation velocity must remain unchanged along the entire length of the channel. Most of these restrictions can be lifted if the model is applied to piecewise linear segments of the channel [*Le Vine and Meneghini*, 1978*a*, *b*]. This approach yields a computationally simple means of accurately calculating the radiation fields from tortuous channels on which the current waveform may change its magnitude, shape, and propagation velocity from segment to segment. (Of course, the induction and electrostatic components of the fields, which become important if the range is not large compared to the overall dimensions of the channel, are still not represented.)

Recently, it has been shown that the original analysis of the transmission-line model by *Uman and McLain* [1970] was not completely correct. *Rubinstein and Uman* [1990] demonstrated that the "turn-on" term defined by *Uman and McLain* [1970, equation (5)] is incomplete. *Rubinstein and Uman* [1990, equation (12)] derived a correction factor that gives the exact expression for the turn-on term. The original formula is an approximation that applies if the channel is oriented perpendicular to the line of sight to the observer or if the propagation velocity is small compared to the speed of light. This approximation is the result of the assumption that the retarded time ($t - R/c$, where R is the distance from the source point to the observer and c is the speed of light) is constant along the channel segment [*Uman and McLain*, 1970, discussion below equation (3)]. In effect, *Rubinstein and Uman* [1990] relaxed this assumption for the turn-on term. However, they said little about the implications of their correction to the application of the transmission-line formula [*Uman and McLain*, 1970, equations (11) and (12)].

In particular, the assumption of constant retarded time requires that the channel segment be perpendicular to the line of sight for most of the interesting cases (e.g., where the current waveform has a steep risetime and the propagation

Paper number 91JD02817.

velocity is high). However, the original transmission-line formula [*Uman and McLain*, 1970, equations (11) and (12)] suggests otherwise because it contains a geometric factor representing the orientation of the channel relative to the observer. *Rubinstein and Uman* [1990] reinforce this erroneous impression by discussing only the turn-on term and not the implications to applications of the transmission-line formula itself [e.g., *Willett et al.*, 1988].

In the present paper we examine the effects of channel orientation on the radiation fields from a propagating current pulse. We show that the transmission-line formulas can be derived in the time domain without resorting to the definition of a turn-on term. This analysis leads to a correction factor essentially identical to that derived by *Rubinstein and Uman* [1990] and also in agreement with formulas for the transmission-line model derived by *Le Vine and Meneghini* [1978*a*, *b*] based on a frequency domain analysis. This correction factor can be significant for channels that are not perpendicular to the line of sight to the observer, such as might occur in models for the stepped leader, branches of a return stroke, or intracloud portions of the discharge.

In the sections to follow, a derivation will be given of the expressions for the radiated electric and magnetic fields from arbitrarily oriented channel segments. (The analysis in the body of the paper applies to an isolated channel segment in an unbounded region. The equations for an arbitrarily oriented segment above a conducting plane are derived in Appendix B.) This will be followed by a discussion of the effects of the correction factor. It will be shown that this factor can resolve some of the direction ambiguity inherent in the original transmission-line formula of *Uman and McLain* [1970, equations (11) and (12)], suggesting that very interesting results might be obtained from multistation measurements like those proposed by *Thomson* [1988].

2. Derivation

In this section a solution is presented for the electromagnetic fields radiated from a short, arbitrarily oriented, straight channel segment in the case when the current on the channel is the traveling wave, $I(t - \hat{l} \cdot \bar{r}'/v)$. The geometry is illustrated in Figure 1*a*. The formal solution is a classic problem which, in the context of the application to lightning, has been developed in the time domain by Uman and colleagues [*Uman and McLain*, 1970; *Uman et al.*, 1975*b*; *Master and Uman*, 1983 (see correction by *Rubinstein and Uman* [1991]); and others] and in the frequency domain by *Le Vine and Meneghini* [1978*a*, *b*]. For example, the solution may be written in the time domain, using vector notation to be general, as follows [*Le Vine and Meneghini*, 1983]:

$$\bar{E}(\bar{r}, t) = -\frac{\mu_0}{4\pi} \int_{\text{segment}} [\dot{I}]\{\hat{l} - (\hat{l} \cdot \nabla R)\nabla R\} \frac{ds'}{R}$$

$$- \frac{\mu_0 c}{4\pi} \int_{\text{segment}} [I]\{\hat{l} - 3(\hat{l} \cdot \nabla R)\nabla R\} \frac{ds'}{R^2}$$

$$- \frac{\mu_0 c^2}{4\pi} \int_{\text{segment}} \left\{ \int_{-\infty}^{t} [I]\{\hat{l} - 3(\hat{l} \cdot \nabla R)\nabla R\}\, dt' \right\} \frac{ds'}{R^3}. \quad (1)$$

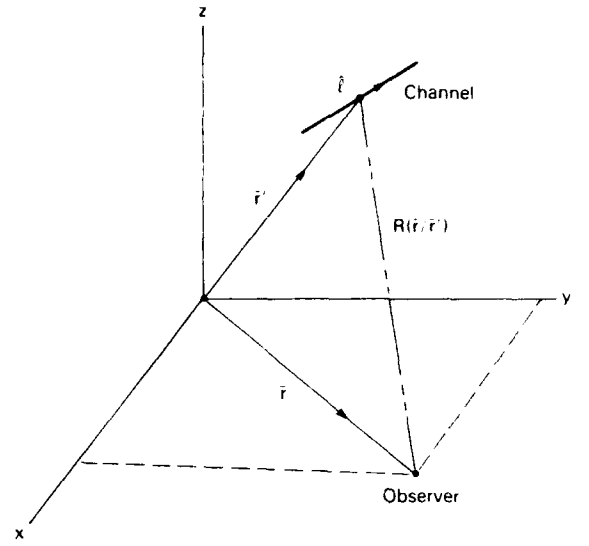

Fig. 1*a*. Geometry used in deriving the transmission-line formulas. The vector $\bar{r}'$ denotes a point on the channel segment, $\bar{r}$ is the position vector locating the observer, and $R(\bar{r}, \bar{r}')$ is the distance between these two points. The ∇R is a unit vector along $R(\bar{r}, \bar{r}')$ pointing from the source point toward the observer.

$$B(r, t) = \frac{\mu_0}{4\pi} \int_{\text{segment}} \left\{ \frac{1}{R}[I] + \frac{1}{c}[\dot{I}] \right\} \frac{\hat{l} \times \nabla R}{R}\, ds'. \quad (2)$$

Notice that the integrals in equations (1) and (2) are line integrals evaluated along the channel segment. The integrations are done in the "primed" coordinate system, and in the notation employed here, ds' denotes a differential length along the segment and ∇R is a unit vector pointing from the source point at $\bar{r}'$ to the observer at $\bar{r}$ (i.e., along $R(\bar{r}, \bar{r}')$ in Figure 1*a*). The brackets ([ ]) in (1) and (2) denote the "retarded" value of the argument (e.g., see equation (5*a*)), and the dot above the brackets denotes a derivative with respect to the argument of the function enclosed by the brackets.

Equations (1) and (2) represent the solution for the electric and magnetic fields due to a transmission-line current pulse propagating in the $\hat{l}$ direction (which is also taken as the positive direction for current flow). They apply to an isolated channel segment (i.e., the effect of a ground plane to represent the earth has not been included). The solution is equivalent to that obtained by Uman and colleagues. For example, (1) and (2) can be reduced to the solution in spherical coordinates for an infinitesimal dipole presented by *Uman et al.* [1975*b*, equations (A6) and (A9) in the appendix] by recognizing that when the current propagates in the z direction (i.e., $\hat{l} = \hat{z}$), as assumed in the paper cited above, one has $(\hat{l} \cdot \nabla R)\nabla R = \cos(\theta)\hat{R}$, $\hat{l} - (\hat{l} \cdot \nabla R)\nabla R = -\sin(\theta)\,\hat{\theta}$, and $\hat{l} \times \nabla R = \sin(\theta)\,\hat{\phi}$, where $\hat{R}$, $\hat{\theta}$, $\hat{\phi}$ are unit vectors along the coordinate axes in a spherical coordinate system. An alternative derivation of (1) and (2), showing that conservation of charge is maintained at the channel end points, has been presented by *Le Vine and Meneghini* [1983].

Unfortunately, even in the simple case of the transmission-line model, general solutions for the integrals in (1) and (2) do not exist, and it is necessary to make approximations. A common approximation, which is useful in the context of radiation from lightning, is to assume that the observer is far

from the channel compared to its length (i.e., $R(\bar{r}, \bar{r}') \gg L$). This is one of the approximations made by *Uman and McLain* [1970] in their original analysis of the stepped leader, and it can be extended to longer channels and to tortuous channels by adopting a piecewise linear model for the channel geometry [e.g., *Le Vine and Meneghini*, 1978*a*]. If R is sufficiently large, then only the terms of lowest order in $1/R$ need be included in (1) and (2), in which case one has

$$\bar{E}(\bar{r}, t) = -\frac{\mu_0}{4\pi} \int_{\text{segment}} [\dot{I}]\{\hat{l} - (\hat{l} \cdot \nabla R)\nabla R\} \frac{ds'}{R} \quad (3)$$

$$\bar{B}(\bar{r}, t) = \frac{\mu_0}{4\pi c} \int_{\text{segment}} [\dot{I}] \frac{\hat{l} \times \nabla R}{R} ds' \quad (4)$$

where

$$[I] = I(t - \hat{l} \cdot \bar{r}'/v - R(\bar{r}, \bar{r}')/c). \quad (5a)$$

Now noting that $(d/ds') = (\hat{l} \cdot \nabla')$ and that $\nabla R = -\nabla' R$, where ∇' is the gradient operator operating on the primed coordinates, one obtains

$$\frac{d}{ds'}[I] = \hat{l} \cdot \nabla'[I] = [\dot{I}]\,\hat{l} \cdot \nabla'(-\hat{l} \cdot \bar{r}'/v - R(\bar{r}, \bar{r}')/c)$$

$$= [\dot{I}](-1/v + \hat{l} \cdot \nabla R/c) \quad (5b)$$

Notice that the effect of $R(\bar{r}, \bar{r}')$ on the retarded time ($\hat{l} \cdot \nabla R/c$ in (5*b*)) is the term missing from the analysis of *Uman and McLain* [1970, equation (7)] and corrected by *Rubinstein and Uman* [1990, where it occurs in a mathematical identity involving the integral of a delta function]. Rearranging (5*b*), we have the relation

$$[\dot{I}] = -\frac{v}{[1 - (v/c)(\hat{l} \cdot \nabla R)]} \frac{d}{ds'}[I] \quad (5c)$$

which can be used in (3) and (4) to rewrite $[\dot{I}]$ in terms of derivatives with respect to the dummy variable of intergration, s'.

For observation points sufficiently far from the channel (i.e., $R(\bar{r}, \bar{r}') \gg L$), it is reasonable to neglect changes in R and ∇R over the length of the channel segment. Replacing R and ∇R by their values at the center of the segment (denoted below by the subscript "0") everywhere except in $[I]$ (see below) and then factoring them out of the integral, one obtains

$$\bar{E}(\bar{r}, t) = \frac{\mu_0 v}{4\pi R_0} \frac{[\hat{l} - (\hat{l} \cdot \nabla R_0)\nabla R_0]}{[1 - (v/c)(\hat{l} \cdot \nabla R_0)]} \int_{\text{segment}} \frac{d}{ds'}[I]\, ds' \quad (6a)$$

$$\bar{B}(\bar{r}, t) = -\frac{\mu_0 v}{4\pi R_0 c} \frac{\hat{l} \times \nabla R_0}{[1 - (v/c)(\hat{l} \cdot \nabla R_0)]} \int_{\text{segment}} \frac{d}{ds'}[I]\, ds' \quad (6b)$$

Finally, performing the integrations indicated in (6*a*) and (6*b*), one obtains

$$\bar{E}(\bar{r}, t) = -\frac{\mu_0 v}{4\pi R_0} \frac{[\hat{l} - (\hat{l} \cdot \nabla R_0)\nabla R_0]}{[1 - (v/c)(\hat{l} \cdot \nabla R_0)]} \cdot \{I(t - t_a) - I(t - t_b)\} \quad (7a)$$

$$\bar{B}(\bar{r}, t) = \frac{\mu_0 v}{4\pi R_0 c} \frac{\hat{l} \times \nabla R_0}{[1 - (v/c)(\hat{l} \cdot \nabla R_0)]} \cdot \{I(t - t_a) - I(t - t_b)\} \quad (7b)$$

where $t_a = \hat{l} \cdot \bar{r}_a'/v + R(\bar{r}, \bar{r}_a')/c$ and $t_b = \hat{l} \cdot \bar{r}_b'/v + R(\bar{r}, \bar{r}_b')/c$ and $\bar{r}_{a,b}'$ represent the ends of the channel segment. Notice that the first term in $t_{a,b}$ represents the time at which the current pulse reaches the indicated end point of the segment, and the second term represents the time required for the radiation to propagate from that end point to the observer. Changes in R between end points have not been neglected in t_a or t_b because they can be important if the current risetime is short, as will be shown in section 3.

Now assuming that $I(t) = 0$ for $t < 0$, notice that for a short period after the radiation initially reaches the observer (i.e., $t > t_a$ but $t < t_b$), the fields in (7*a*) and (7*b*) are proportional to the current at the initial end point ($\bar{r}_a'$) of the channel. That is, in the time interval, $t_a < t < t_b$, (7*a*) and (7*b*) are

$$\bar{E}(\bar{r}, t) = -\frac{\mu_0 v}{4\pi R_0} \frac{[\hat{l} - (\hat{l} \cdot \nabla R_0)\nabla R_0]}{[1 - (v/c)(\hat{l} \cdot \nabla R_0)]} I(t - t_a) \quad (8a)$$

$$\bar{B}(\bar{r}, t) = \frac{\mu_0 v}{4\pi R_0 c} \frac{\hat{l} \times \nabla R_0}{[1 - (v/c)(\hat{l} \cdot \nabla R_0)]} I(t - t_a). \quad (8b)$$

This is the important result noticed by *Uman and McLain* [1970] that generated interest in estimating the current in lightning discharges indirectly from observation of the radiated electromagnetic fields. (Notice, however, that the proportionality constant involves the velocity of propagation, v, distance, R_0, and orientation of the segment, $\hat{l}$, all of which must also be determined in order to obtain a valid measurement of $I(t)$.)

Equations (7*b*) and (8*b*) for a single channel segment in a boundary-free region correspond to the transmission-line formulas obtained by *Uman and McLain* [1970, equations (11) and (12)] for a vertically oriented channel and its image in a conducting plane. Aside from the generalization made here to include arbitrarily oriented channel segments, however, (7*b*) and (8*b*) differ from the results presented by *Uman and McLain* [1970] in two important respects. The first is the presence of the multiplicative factor $[1 - (v/c)(\hat{l} \cdot \nabla R)]^{-1}$, which is not present in the expressions derived by *Uman and McLain* [1970]. The second is the dependence of the time delays, $t_{a,b}$, on the time required for the electromagnetic radiation to propagate from the ends of the segment to the observer (i.e., the terms $R(\bar{r}, \bar{r}_a')/c$ and $R(\bar{r}, \bar{r}_b')/c$ in the expressions for t_a and t_b). These terms are not present in the expressions presented by *Uman and McLain* [1970; see equations (11) and (12) and the discussion below equation (10) where "τ_v" is defined). Both of these differences result from our relaxation of the assumption of constant retarded time.

In order to gain insight into the nature of (7) and (8) and to better compare with the transmission-line formula obtained by *Uman and McLain* [1970], equations (7) and (8) will be examined in section 3 in the special case of a vertical channel segment. It will be shown in this example that the differences mentioned above can be quite significant.

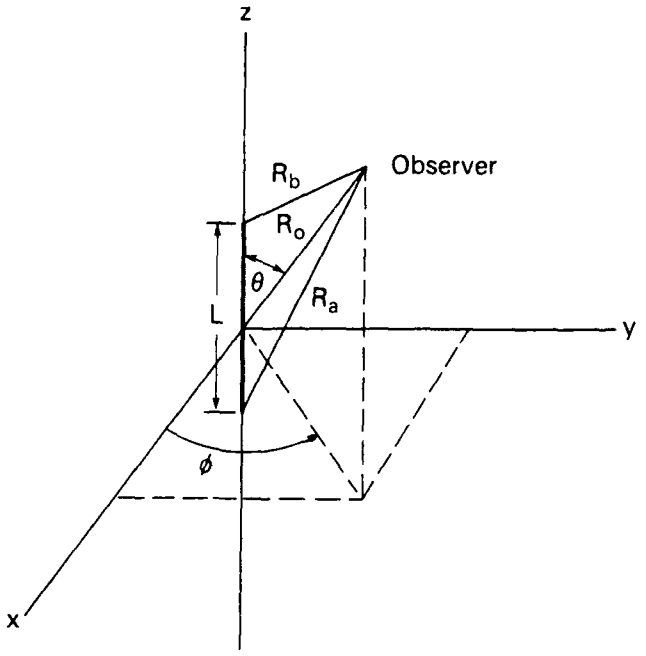

Fig. 1*b*. Geometry used to compute an approximation for the time delays t_a and t_b that is valid when $R_0 \gg L$. This figure also defines the spherical coordinate system introduced in section 3.

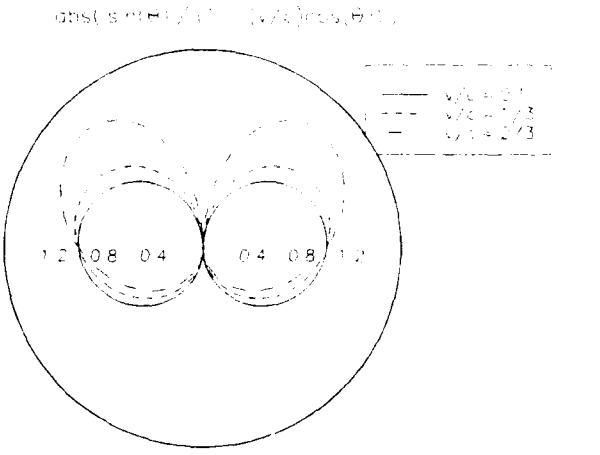

Fig. 2. Polar plot of the absolute value of the geometric factor, $\sin(\theta)/[1 - (v/c)\cos(\theta)]$, for several different values of v/c. The angle θ is zero along the vertical axis (pointing up) and increases in the clockwise direction (see also Figure 1*b*).

3. EXAMPLE

Vertical Channel Segment

In order to more readily visualize (7*a*) and (7*b*) above, consider the solutions expressed in a spherical coordinate system with its origin at the center of the channel segment and oriented so that the current propagates in the direction of the positive z axis, as illustrated in Figure 1*b*. The observer is located at the point R, θ, ϕ. (Since no boundaries are present, this represents a completely general case. The solutions for an arbitrarily oriented channel segment above a conducting plane are worked out in Appendix B.) In this case, one finds that $\nabla R_0 = \hat{R}$ and $\hat{l} = \hat{z} = \cos(\theta)\hat{R} - \sin(\theta)\hat{\theta}$, and it is easily shown that $\hat{l} - (\hat{l} \cdot \nabla R_0)\nabla R_0 = -\sin(\theta)\hat{\theta}$ and that $\hat{l} \times \nabla R_0 = \sin(\theta)\hat{\phi}$, where $\hat{R}$, $\hat{\theta}$, and $\hat{\phi}$ are the orthogonal unit vectors in the new coordinate system. Using these expressions in (7*a*) and (7*b*), one obtains

$$\bar{E}(\bar{r}, t) = \frac{\sqrt{\mu_0/\epsilon_0}}{4\pi R_0}(v/c)\frac{\sin(\theta)\hat{\theta}}{[1 - (v/c)\cos(\theta)]} \cdot [I(t - t_a) - I(t - t_b)] \qquad (9a)$$

$$\bar{B}(\bar{r}, t) = \frac{\mu_0}{4\pi R_0}(v/c)\frac{\sin(\theta)\hat{\phi}}{[1 - (v/c)\cos(\theta)]} \cdot [I(t - t_a) - I(t - t_b)] \qquad (9b)$$

Notice that the fields in (9*a*) and (9*b*) are orthogonal to each other and to the line of sight, $\hat{R}$, from the channel segment to the observer. Also notice that the ratio of the magnitude of the electric and magnetic fields is the speed of light in vaccum (i.e., $[\bar{E} \cdot \hat{\theta}/\bar{B} \cdot \hat{\phi}] = c$). These are properties that one expects to find in the radiation components of electric and magnetic fields.

Both fields in (9*a*) and (9*b*) are proportional to the ratio $\sin(\theta)/[1 - (v/c)\cos(\theta)]$. In the equivalent result obtained by *Uman and McLain* [1970, equations (11) and (12)], the magnetic field, $\bar{B}(\bar{r}, t)$, is proportional only to $\sin(\theta)$, and the factor $[1 - (v/c)\cos(\theta)]^{-1}$ is not present. In order to illustrate the significance of this difference the absolute value of the geometry factor $\sin(\theta)/[1 - (v/c)\cos(\theta)]$ has been plotted in Figure 2 as a function of θ for several values of (v/c).

Notice that when $v/c \ll 1$, the expression $[1 - (v/c)\cos(\theta)] \cong 1$, in which case (9*b*) reduces to the result obtained by *Uman and McLain* [1970] (except for a factor of 2 introduced because they included the effect of a perfectly conducting ground plane in their analysis (see Appendix B)). In this case, the radiation pattern is identical to the classical pattern of radiation from a dipole [e.g., *Jackson*, 1966]. However, as the ratio v/c increases, the radiation pattern changes, becoming peaked and tilted toward the direction of propagation of the current pulse. This is an effect seen in traveling wave antennas [e.g., *Jordan and Balmain*, 1968].

Of course, the magnitude of the fields in (9*a*) and (9*b*) also depends directly on the ratio (v/c), as shown by *Uman and McLain* [1970]. That is, not only does the radiation tend to peak in the direction of propagation along the channel segment as $v/c \to 1$ but also the magnitude of the radiation itself increases. This is illustrated in Figure 3, where the absolute value of the quantity $(v/c)\sin(\theta)/[1 - (v/c)\cos(\theta)]$ has been plotted for the same values of v/c as used in generating Figure 2.

Finally, note that the radiation patterns in Figures 2 and 3 are rotationally symmetric about the z axis because in the geometry being treated here, there is no dependence on the coordinate, ϕ.

In addition to the explicit dependence of the fields on the segment-observer geometry, as described above, there is also an implicit dependence included in (9*a*) and (9*b*) in the factor, $I(t - t_a) - I(t - t_b)$. This is demonstrated in Appendix A, where it is shown that when $L/R_0 \ll 1$, one obtains

$$t_a = R_0/c - \frac{L}{2v}[1 - (v/c)\cos(\theta)] \qquad (10a)$$

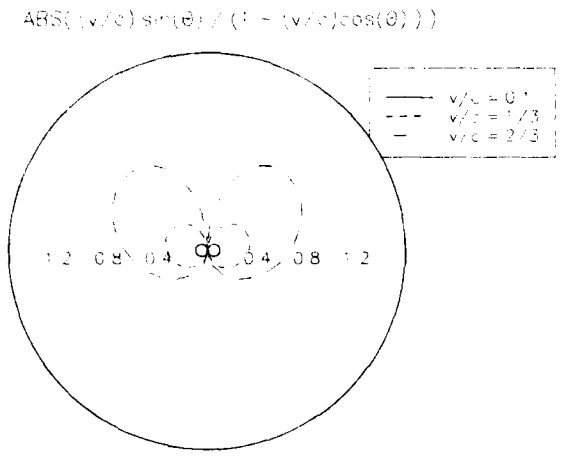

Fig. 3. Polar plot of the absolute value of the factor, $[(v/c) \sin (\theta)]/[1 - (v/c) \cos (\theta)]$, for several different values of v/c. The angle θ is zero along the vertical and increases clockwise.

$$t_b = R_0/c + \frac{L}{2v}[1 - (v/c) \cos (\theta)] \qquad (10b)$$

and we define

$$\tau \equiv t_b - t_a = (L/v)[1 - (v/c) \cos (\theta)] \qquad (10c)$$

In (10a), (10b), and (10c), L is the length of the channel segment.

As mentioned earlier, t_a and t_b consist of the time required for the current pulse to propagate to the appropriate end of the segment, plus the time required for electromagnetic radiation to cover the distance from the respective end point to the observer. Since, in general, neither of these times is the same for the two end points, one obtains the nonzero net time difference τ defined in (10c). The value of τ is the difference in the retarded times associated with the arrival of the current pulse at the two end points of the channel segment.

Notice that the first term in τ (i.e., L/v) is just the time required for the current to propagate from one end of the channel to the other end. In the original work on the transmission-line model only this term was taken into account. As a result, *Uman and McLain* [1970, see equations (11) and (12) and the discussion below equation (10) where τ_v is defined) ignored the dependence on the angle θ contained in the second term in (10c) (i.e., $-(L/c) \cos \theta$).

The effect that this implicit dependence on the channel-observer geometry can have on the radiation depends on the shape of the current waveform, $I(t)$. In particular, when $I(t)$ has a rapid risetime, as is typical of the current in return strokes, small variations in τ can cause large changes in the observed fields. In this case, (9) and (10) can be significantly different from those in which $\tau_v = L/v$).

To illustrate this, the difference $I(t - t_a) - I(t - t_b)$ has been plotted in Figure 4b for several different values of the angle θ. To generate these examples, it has been assumed that $L = 100$ m and $v = 10^8$ m/s. An exponential model has been chosen for the current waveform, as illustrated in Figure 4a: $I(t) = I_0$ [exp $(-at)$ − exp $(-bt)$], where $a = 2 \times 10^4$ s^{-1} and $b = 3.5 \times 10^6$ s^{-1}. This is the current waveform suggested by *Bruce and Golde* [1941] with parameters suggested by *Dennis and Pierce* [1964] to describe

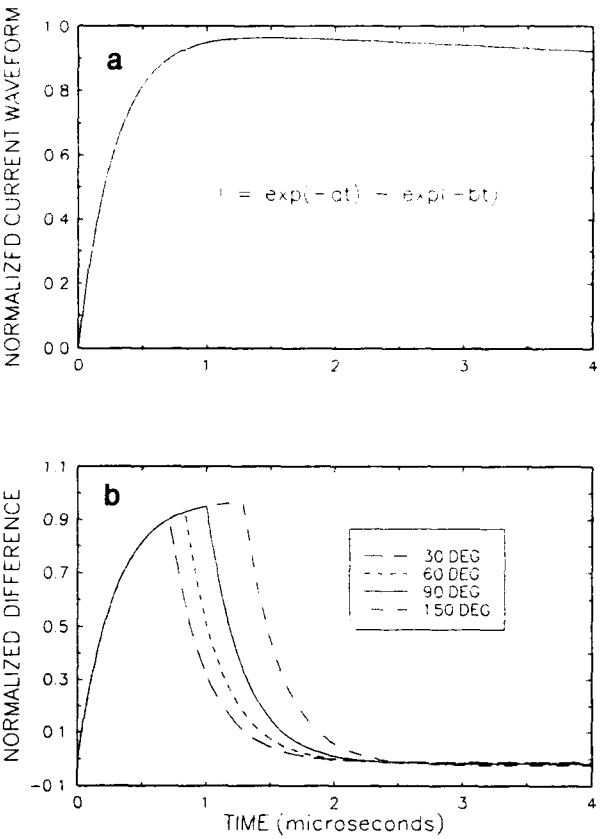

Fig. 4. (*a*) The current waveform used in (*b*) to compute the factor $[I(t) - I(t - \tau)]/I_0$ for various values of θ. The θ-dependent element of this expression is $\tau = (L/v)[1 - (v/c) \cos (\theta)]$ (equation (10c)). The solid curve ($\theta = 90°$) corresponds to the result obtained by *Uman and McLain* [1970] for all values of θ.

return strokes, except that b has been modified to reflect modern measurements that suggest a more rapid risetime [e.g., *Weidman and Krider*, 1980, 1982].

Equation 10c shows that τ is a minimum at $\theta = 0°$ and increases to a maximum at $\theta = 180°$. The consequence is evident in the four curves in Figure 4b. For example, the curve for $\theta = 150°$ has the largest peak value because the longer retarded time difference permits $I(t - t_a)$ to grow more before the term $-I(t - t_b)$ arrives and begins to cancel it. Similar results would be obtained for other choices of L, v and $I(t)$, although changing the current waveform would change the specific shape of the curves.

As described above, the expression $[1 - (v/c) \cos (\theta)]$ affects the radiated fields in two ways: explicitly through the geometry-dependent factor $\sin (\theta)/[1 - (v/c) \cos (\theta)]$, as illustrated in Figures 2 and 3, and implicitly through the difference $I(t - t_a) - I(t - t_b)$, as illustrated in Figure 4. The combined effect of these two terms is shown in Figure 5, where the complete solution has been plotted for several values of θ, using the parameters described above. For this purpose a normalized field magnitude, $F(\theta, t)$, has been defined as follows:

$$F(\theta, t) = |\bar{E}(\bar{r}, t)| \Big/ \left[\frac{\sqrt{\mu_0/\varepsilon_0}}{4\pi R_0} (v/c) I_0\right]$$

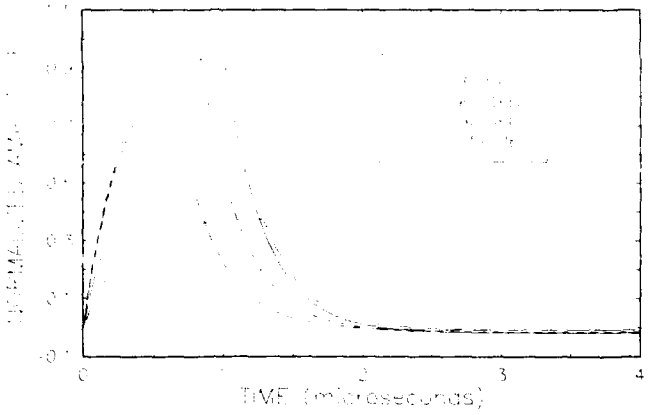

Fig. 5. Complete solution (equations (9) and (10)), using the current waveform of Figure 4*a*, for several different angles θ. The normalized field $F(\theta, t)$, defined by equation (11), has been plotted.

$$= |\bar{B}(\bar{r}, t)| \Big/ \left[\frac{\mu_0}{4\pi R_0}(v/c) I_0\right]. \qquad (11)$$

Comparing Figures 2 and 4*b*, it is clear that the explicit and implicit contributions affect the received fields in different ways. The implicit dependence results in an increase in the amplitude as θ increases, because the time delay is increased (Figure 4*b*). On the other hand, the effect of the explicit dependence (Figure 2) is to increase the amplitude to a peak near $\theta = 60°$ and then to decrease it with further increases in angle. It is clear from Figure 5 that the explicit dependence dominates in this case, resulting in a net decrease in amplitude for angles greater than about 60°.

Equations (9) and (10) are equivalent to the results obtained by *Uman and McLain* [1970, equations (11) and (12)] when $\theta = 90°$, because $[1 - (v/c) \cos(\theta)] = 1$ in this case. However, for other values of θ the two can be quite different. This is illustrated in Figure 6, where the two solutions have been plotted together. (Uman and McLain's solution has been divided by 2 to compensate for the effect of the conducting plane in their analysis.) In each case, the normalized field, defined in (11), has been plotted after dividing by $\sin(\theta)$, a factor common to both solutions.

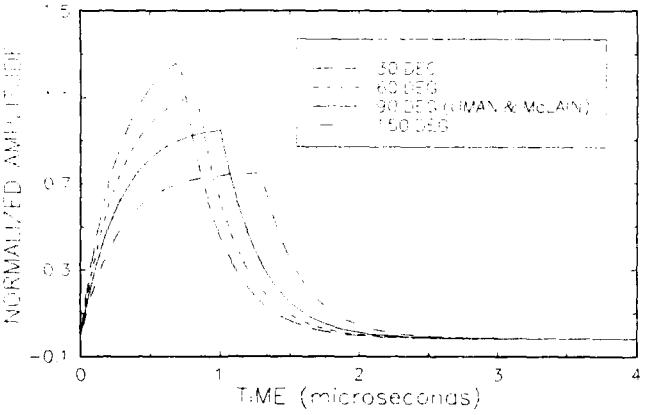

Fig. 6. Comparison of the *Uman and McLain* [1970] solution, represented by the solid curve for all θ and equations (9) and (10) for several different angles, using the current waveform of Figure 4*a*. $F(\theta, t)/\sin\theta$ has been plotted to remove the common factor from both normalized fields. The two solutions are the same when $\theta = 90°$.

The Uman and McLain result corresponds to the solid curve in Figure 6, and it applies for all θ since $\sin(\theta)$ is the only θ dependence in their solution. Dividing (9*a*) and (9*b*) by $\sin(\theta)$ leaves the implicit and explicit dependences on $[1 - (v/c) \cos(\theta)]$ added by the present analysis. Our result has been plotted for several values of θ, using the parameters described above. It is clear from Figure 6 that (9*a*) and (9*b*) can differ significantly from the Uman and McLain solution for values of θ other than 90°.

4. Apparent Singularity

In addition to the characteristics of (7) and (9) pointed out above, notice that when $v/c = 1$, it is possible for the expression $[1 - (v/c)(\hat{l} \cdot \nabla R_0)]$ in (7*a*) and (7*b*) (or equivalently, the expression $[1 - (v/c) \cos(\theta)]$ in (9*a*) and (9*b*)) to be zero. This happens when the observer is along the axis of the channel segment in the direction of propagation of the current waveform (i.e., $\hat{l} = \nabla R_0$ or $\theta = 0$). At first glance it appears that the fields are unbounded in this case, since $\sin(\theta)/[1 - \cos(\theta)]$ blows up as θ goes to zero. However, the singularity is only apparent, and both fields actually go to zero along the axis of the segment.

To see this, again consider a spherical coordinate system with its origin at the center of the channel segment and oriented such that $\hat{l} = \hat{z}$. It is desired to examine the fields (equations (9*a*) and (9*b*)) near the axis ($\theta = 0$) in the special case $v/c = 1$. Since $v = c$, one can always get close enough to the axis so that the retarded time difference, τ (equation (10*c*)), is small, no matter how long the channel segment becomes (i.e., whatever the magnitude of L/c). Assuming that τ is small, and using $t_a = R_0/c - \tau/2$ and $t_b = R_0/c + \tau/2$ from (10*a*), (10*b*), and (10*c*), we can expand $I(t - t_a)$ and $I(t - t_b)$ in power series about $\hat{t} \equiv t - R_0/c$. To first order in τ this yields

$$I(t - t_a) - I(t - t_b) \cong \tau \frac{d}{dt} I(t)\Big|_{t=\hat{t}} \qquad (12a)$$

Hence close to the axis the normalized field (equation (11) becomes

$$F(\theta, t) = \frac{\sin(\theta)}{[1 - (v/c) \cos\theta]} [I(t - t_a) - I(t - t_b)]/I_0$$

$$\cong (L/vI_0) \sin(\theta) \frac{d}{dt} I(t)\Big|_{t=\hat{t}} \qquad (12b)$$

which goes to zero as $\theta \to 0$. Thus both $\bar{E}(\bar{r}, t)$ and $\bar{B}(\bar{r}, t)$ go to zero along the axis of the channel segment, and there is, in fact, no singularity.

One can reach the same conclusion using the following argument. Notice that when $\theta = 0$ and $v/c = 1$, the current pulse leaving the initial end of the channel segment (i.e., at $\bar{r}' = \bar{r}'_a$) and the electromagnetic field radiated from this end (i.e., the term corresponding to $I(t - t_a)$ in (9*a*) and (9*b*)) propagate toward the observer along the same ray path and at the same velocity. Consequently, in this special case they both reach the other end of the segment at the same time. When the current pulse reaches this end of the segment, a second pulse of radiation is emitted (the term associated with

$-I(t - t_b)$ in (9a) and (9b). The radiation from this end is equal in amplitude but opposite in sign to the radiation arriving from the initial end and cancels the arriving radiation. Hence the net electromagnetic field radiated to the observer is zero. In effect, the two singularities in (9a) and (9b) cancel each other, leaving the fields bounded.

5. Very Short Segment

The radiated fields (equations (9a) and (9b)) reduce to an interesting special form in the case of a very short channel segment, as might be appropriate, for example, in modeling radiation from an individual step in the stepped leader process. Assume that the segment is sufficiently short that $L/v \ll \tau_r$, where τ_r is the risetime of the current pulse. From (10c) the retarded time difference $\tau \ll \tau_r$, because $[1 - (v/c) \cos \theta] < 2$ for any $v < c$. Now expand $I(t)$ in a power series in τ, as done in (12a) above, keeping only terms of lowest order in τ. Inserting (12b) into (9a) and (9b), one obtains

$$\bar{E}(\bar{r}, t) = \hat{\theta} \frac{\sqrt{\mu_0/\varepsilon_0}}{4\pi R_0} (L/c) \sin(\theta) \frac{d}{dt} I(t)\Big|_{t=\hat{t}} \quad (13a)$$

$$\bar{B}(\bar{r}, t) = \hat{\phi} \frac{\mu_0}{4\pi R_0} (L/c) \sin(\theta) \frac{d}{dt} I(t)\Big|_{t=\hat{t}}. \quad (13b)$$

As one would expect in this limit, the radiation pattern is identical to that of a classical dipole [*Jackson*, 1966; *Uman et al.*, 1975*b*, equations (A6) and (A8)], regardless of the ratio v/c. Also notice that the radiation is directly proportional to the derivative of the current waveform, rather than being proportional to the current waveform itself as is the case (at least initially) with a longer segment (i.e, (7) or (9)). Finally, notice that in this case, the magnitude of the fields is no longer proportional to the velocity of propagation of the current, v, but is now directly proportional to the length, L, of the channel segment.

Also notice that for this very short segment the dependence on $[1 - (v/c) \cos(\theta)]$ has entirely disappeared. As the channel element gets shorter and shorter, the explicit and implicit dependences on this expression become nearly equal and tend to cancel each other, indicating both both dependences are needed for a self-consistent solution. This cancellation is illustrated in Figure 7, where the normalized fields have been plotted (using (9) and (11)) for several values of θ and for decreasing values of the element length, L. (As in Figure 6, $F(\theta, t)/\sin(\theta)$ has been plotted to emphasize the effects of the expression $[1 - (v/c) \cos(\theta)]$.) Notice the clear dependence on θ for $L = 20$ m and the obvious lack of dependence on this factor when $L = 0.8$ m. It is also apparent from Figure 7 that the peak amplitude attained by the fields is decreasing in proportion to L.

Finally, notice that in order for (13a) and (13b) to be applicable to lightning, it is not sufficient that the channel be short. In particular, in order to neglect higher order terms in the power series expansion, it was necessary to assume that L/v was small compared to τ_r. Thus at least in the context of a transmission-line model, use of the dipole approximation requires that the time required for the current pulse to propagate the length of the channel segment be small compared to the risetime of the current waveform itself. This is in agreement with the earlier result of *Krider and Radda* [1975].

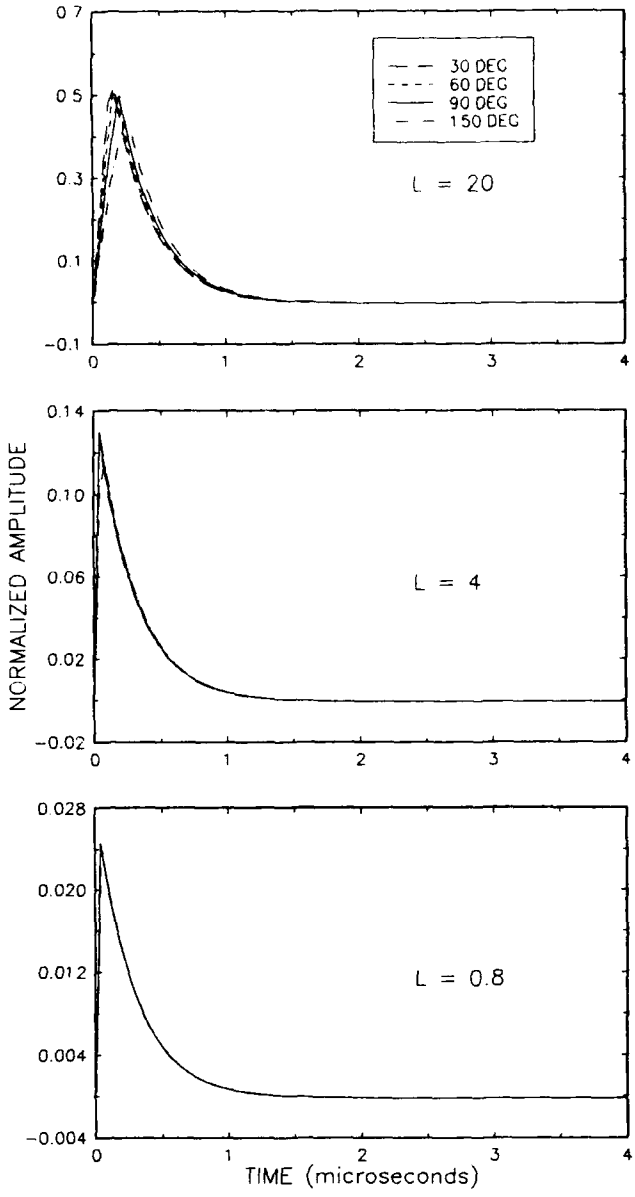

Fig. 7. Effect of channel length, L, on the radiation from a straight segment. For each value of L, $F(\theta, t)/\sin\theta$ has been plotted (based on equations (9), (10), and (11)) for several different angles, θ, using the current waveform of Figure 4a. Note that Figure 6 shows the same function for $L = 100$ m.

6. Consequences for Remote Sensing

Recently, an experiment has been proposed by *Thomson* [1988] to use wideband, multistation measurements of the radiated fields to determine the location, channel orientation, current waveform, and velocity-current product for certain processes in the lightning discharge. It has generally been assumed that the radiation fields only contain information about the magnitude of the velocity-current product and no information on the direction of propagation of the current waveform along any given channel segment. This is because in the *Uman and McLain* [1970, equations (11) and (12)]

TABLE 1. Ambiguity in Measurement of Electric Field

Direction of Propagation	Current		Sign of $\vec{E}_S(t)$	Factor $[1 - (v/c)(\hat{l} \cdot \nabla R_0)]$
	Sign	Direction		
↑	+	↑	−	$[1 - (v/c) \cos(\theta)]$
↑	−	↓	+	$[1 - (v/c) \cos(\theta)]$
↓	+	↓	+	$[1 + (v/c) \cos(\theta)]$
↓	−	↑	−	$[1 + (v/c) \cos(\theta)]$

version of the transmission-line formulas, current and propagation velocity appear only as a product. However, in the formulas derived in the present paper, the correction factor $[1 - (v/c)(\hat{l} \cdot \nabla R)]^{-1}$ resolves this ambiguity and provides the possibility that current and velocity might be individually determined with suitable multistation measurements.

The nature of the ambiguity is illustrated in Table 1 for the special case of a vertical channel over a perfectly conducting ground plane (see Appendix B). The first column in the table indicates the direction of propagation of the current waveform on this channel. This is the direction of the unit vector, $\hat{l}$. (The velocity, v, is always a positive number in the formulation in this paper.) The second column in Table 1 indicates the sign of the current flowing in the direction indicated in the first column. A plus sign means positive charge moving in the direction of the arrow, and a minus means negative charge moving in this direction. The third column indicates the direction of the current vector, $\vec{i}(\vec{r}', t) = \hat{l}I(\vec{r}', t)$, determined by the entries in the first two columns.

The fourth column in Table 1 gives the sign of the vertical component of electric field measured on the surface, given the conditions indicated in the first two columns. Here a plus sign means that the electric field points vertically upward, away from the surface (as though there were negative charges aloft), and a minus means that the electric field points downward, toward the surface. The signs indicated in this column are obtained directly from equation (B5).

Notice that each sign in the fourth column of Table 1 appears twice. For example, positive current propagating upward and negative current propagating downward both yield negative electric fields on the surface. Throughout the table the direction of the electric field is opposite to the direction of the current vector, indicated by the arrows in the third column, as one would expect from (1). Thus it is clear that one cannot, based on the sign of the electric field alone, determine the direction of propagation of the current waveform.

In the original version of the transmission-line formulas [e.g., *Uman and McLain*, 1970; *Thomson*, 1988], cases with electric fields of the same sign in our table also have the same magnitude, and therefore are indistinguishable. However, in the solution presented here, the correction factor $[1 - (v/c)(\hat{l} \cdot \nabla R_0)]^{-1}$ introduces an additional dependence on the direction of propagation, $\hat{l}$, that resolves this ambiguity. The form that this correction factor takes in each of the four cases is indicated in the last column of Table 1.

Notice that the correction factor is different in the previously ambiguous cases, because the sign of $\hat{l} \cdot \tau R_0$ is different. Thus the amplitude of the electric field will, in general, be different in these cases. Since this amplitude difference depends on the angle θ, it may be possible, by making measurements at several locations having different values of $\cos(\theta)$, to distinguish upward and downward propagation of the current waveform. Furthermore, since the correction factor also depends on the velocity, v, it may even be possible to separately determine the velocity of propagation and the magnitude of the current. Such a possibility would be of great interest, for example, in the case of leader steps, for which neither the velocity nor the direction of propagation is known [e.g., *Krider and Radda*, 1975].

7. Discussion

Equations (7*a*) and (7*b*) are approximate expressions that apply when the observation point is far from the channel segment. However, the presence of the factor $[1 - (v/c)(\hat{l} \cdot \nabla R_0)]^{-1}$ does not appear to be a consequence of this approximation. In particular, it is possible to obtain an exact solution (i.e., no approximations needed to evaluate the integrals in (1) and (2)) in the special case $v = c$ [*Le Vine and Meneghini*, 1978*b*], and the formulas obtained in this case, contain the factor $[1 - (\hat{l} \cdot \nabla R_0)]^{-1}$. This latter solution is valid independent of distance from the channel; consequently, the factor $[1 - (\hat{l} \cdot \nabla R_0)]^{-1}$ is present in the radiation component of the fields at all distances $R(\vec{r}, \vec{r}_0')$ even very close to the channel. Furthermore, the exact solution does not appear to be singular in v/c because letting $R(\vec{r}/\vec{r}_0') \to \infty$ in this solution yields (7*a*) and (7*b*) with v replaced by c [*Le Vine and Meneghini*, 1978*b*].

Finally, notice that the factor $[1 - (v/c)[\hat{l} \cdot \nabla R_0)]^{-1}$ is not unusual, appearing in other applications of Maxwell's equations. For example, this factor is present in the theory for traveling wave antennas [e.g., *Jordan and Balmain*, 1968] and also appears in the expression for the Lienard-Wiechert potentials used to describe radiation from a moving charge [*Jones*, 1964; *Meneghini*, 1984]. This factor also appears in the correction that *Rubinstein and Uman* [1990] made to the original theory of *Uman and McLain* [1970], as part of their analysis of the turn-on term.

In summary, the conventional formulas used to relate current and radiation fields in the transmission-line model must be modified to include the amplitude factor $[1 - (v/c)(\hat{l} \cdot \nabla R_0)]^{-1}$. It is clear from Figure 2 that this factor can be significant in applications to radiation from lightning. When $v \ll c$, this factor is nearly unity, and the radiation pattern reduces to the classical pattern of radiation from a dipole. In this case, the original formulas due to *Uman and McLain* [1970] are applicable. This correction factor is also likely to be very nearly unity when considering radiation from near the base of return stroke channels to an observer on the ground, a case in which the channel is close to vertical, hence perpendicular to the line of sight (i.e., $\hat{l} \cdot \nabla R_0 \cong 0$). However, for radiation from elevated points on the channel and/or from channel segments of arbitrary orientation, as might be encountered in modeling radiation from leader steps, channel branches or intracloud processes, $\hat{l} \cdot \nabla R_0 \neq 0$ in general, and the correction factor $[1 - (v/c)(\hat{l} \cdot \nabla R_0)]^{-1}$ can be significant.

Appendix A

Consider a channel segment of length L oriented along the z axis of a spherical coordinate system as indicated in Figure

1*b*. The origin is at the center of the segment. The purpose of this appendix is to compute the time delays $t_a = R_a/c - L/(2v)$ and $t_b = R_b/c + L/(2v)$ in the special case $R_0 \gg L$. Thus letting θ be the angle R_0 makes with the z axis, one obtains the following expressions from standard trigonometric rules:

$$R_a = R_0\sqrt{1 + (L/R_0)\cos(\theta) + (L/2R_0)^2} \quad \text{(A1)}$$

$$R_b = R_0\sqrt{1 - (L/R_0)\cos(\theta) + (L/2R_0)^2} \quad \text{(A2)}$$

Expanding the square root in a power series keeping only the first order terms in the small parameter (L/R_0), one obtains

$$R_a \cong R_0 + (L/2)\cos(\theta) \quad \text{(A3)}$$

$$R_b \cong R_0 - (L/2)\cos(\theta) \quad \text{(A4)}$$

The error is of the order of L^2/R_0. Using (A3) and (A4), it follows that

$$t_a = -L/(2v) + R_a/c \cong R_0/c - \frac{L}{2v}[1 - (v/c)\cos(\theta)] \quad \text{(A5)}$$

$$t_b = +L(2v) + R_b/c \cong R_0/c + \frac{L}{2v}[1 - (v/c)\cos(\theta)]. \quad \text{(A6)}$$

Appendix B

Since most applications to lightning are for measurements made on the surface of the Earth, equations are derived in this appendix for the radiation fields seen by an observer on the surface when the source is over a perfectly conducting ground plane. This problem is solved by applying the method of images. In particular, the solutions are obtained by adding to (1) and to (2) the contribution due to an image current, $i_I(\bar{r}_I', t) = -I(t - \hat{l}_I \cdot \bar{r}_I'/v)$, where $\bar{r}_I' = \bar{r}' - 2z'\hat{z}$ and $\hat{l}_I = [\hat{l} - 2(\hat{l} \cdot \hat{z})\hat{z}]$. The solutions for the fields due to the image current follow the procedure outlined in (3) through (7) in the text and are added to the solutions already presented there.

When the observer is on the surface, the solutions simplify greatly because on the surface the electric field has only a component perpendicular to the surface and the magnetic field has only a component tangential to the surface. The solutions in this case can be written quite simply in terms of (7*a*) and (7*b*). Letting $\hat{n}$ denote a unit vector perpendicular to the surface and letting $\bar{E}_s(\bar{r}, t)$ and $\bar{B}_s(\bar{r}, t)$ denote the fields on the surface, one obtains

$$\bar{E}_s(\bar{r}, t) = 2[\hat{n} \cdot \hat{E}(\bar{r}, t)]\hat{n}$$

$$= -\frac{\mu_0 v}{2\pi R_0}\frac{\{[\nabla R_0 \times (\hat{n} \times \nabla R_0)] \cdot \hat{l}\}\hat{n}}{[1 - (v/c)(\hat{l} \cdot \nabla R_0)]}[I(t - t_a) - I(t - t_b)] \quad \text{(B1)}$$

$$\bar{B}_s(\bar{r}, t) = 2[\hat{n} \times \bar{B}(\bar{r}, t)] \times \hat{n}$$

$$= \frac{\mu_0 v}{2\pi R_0 c}\frac{[\hat{n} \times (\hat{l} \times \nabla R_0)] \times \hat{n}}{[1 - (v/c)(\hat{l} \cdot \nabla R_0)]}[I(t - t_a) - I(t - t_b)] \quad \text{(B2)}$$

where $\bar{E}(\bar{r}, t)$ and $\bar{B}(\bar{r}, t)$ are the solutions given in (7*a*) and (7*b*), respectively, and where (B1) is obtained from (7*a*) with the vector identity $\bar{a} \times (\bar{b} \times \bar{c}) - \bar{b}(\bar{a} \cdot \bar{c}) - \bar{c}(\bar{a} \cdot \bar{b})$.

In order to compare with other forms of the solution that have appeared in the literature, consider a spherical coordinate system with its origin at the center of the channel segment, as in section 3, but oriented so that its z axis is perpendicular to the surface ($\hat{n} = \hat{z}$). Then, noting that $\nabla R_0 \times [\hat{n} \times \nabla R_0] = -\sin(\theta)\hat{\theta}$, (B1) and (B2) can be written

$$\bar{E}_s(\bar{r}, t) = \frac{\mu_0 v}{2\pi R_0}\frac{\sin(\theta)(\hat{\theta} \cdot \hat{l})\hat{z}}{[1 - (v/c)(\hat{l} \cdot \nabla R_0)]} \cdot [I(t - t_a) - I(t - t_b)] \quad \text{(B3)}$$

$$\bar{B}_s(\bar{r}, t) = \frac{\mu_0 v}{2\pi R_0 c}\frac{[\hat{z} \times (\hat{l} \times \nabla R_0)] \times \hat{z}}{[1 - (v/c)(\hat{l} \cdot \nabla R_0)]} \cdot [I(t - t_a) - I(t - t_b)]. \quad \text{(B4)}$$

Note that the angle θ is larger than 90° when the real source is above the ground plane.

In addition, if the channel segment is oriented parallel to the z axis (i.e., $\hat{l} = \pm\hat{z}$), then our spherical coordinate system becomes identical to that of Figure 1*b*, and the results simplify further (e.g., $\hat{l} \cdot \nabla R_0 = \pm\cos(\theta)$, $[\hat{z} \times (\hat{l} \times \nabla R_0)] \times \hat{z} = \pm\sin(\theta)\hat{\phi}$, and $\hat{l} \cdot \hat{\theta} = \mp\sin(\theta)$). One obtains

$$\bar{E}_s(\bar{r}, t) = \mp\frac{\mu_0 v}{2\pi R_0}\frac{\sin^2(\theta)\hat{z}}{[1 \mp (v/c)(\cos\theta)]} \cdot [I(t - t_a) - I(t - t_b)] \quad \text{(B5)}$$

$$\bar{B}_s(\bar{r}, t) = \pm\frac{\mu_0 v}{2\pi R_0 c}\frac{\sin(\theta)\hat{\phi}}{[1 \mp (v/c)(\cos\theta)]} \cdot [I(t - t_a) - I(t - t_b)] \quad \text{(B6)}$$

Here the upper sign applies to an upward propagating current pulse and the lower to downward propagation. (Recall, however, that the positive direction for current flow is taken as the propagation direction, so that the fields do not reverse sign unless the current flow reverses direction.) Except for the explicit correction factor $[1 \mp (v/c)(\cos\theta)]^{-1}$ and the additional θ dependence implicit in t_a and t_b, (B6) is identical to that derived by *Uman and McLain* [1970].

Acknowledgments. This work was begun while the second author was a National Research Council Research Associate at the NASA Goddard Space Flight Center. Funding was provided by NASA.

References

Bruce, C. E. R., and R. H. Golde, The lightning discharge, *J. Inst. Electr. Eng. London*, *88*(II), 487–505, 1941.

Dennis, A. S., and E. T. Pierce, The return stroke of the lightning flash to earth as a source of VLF atmospherics, *J. Res. Natl. Bur. Stand., Sect. D*, *68*, 77–794, 1964.

Jackson, J. D., *Classical Electrodynamics*, 5th ed., chap. 9, John Wiley, New York, 1966.

Jones, D. S., *The Theory of Electromagnetism*, chap. 3, Pergamon, New York, 1964.

Jordan, E. C., and K. G. Balmain, *Electromagnetic Waves and Radiating Systems*, chap. 11, Prentice-Hall, Englewood Cliffs, N. J., 1968.

Krider, E. P., and G. J. Radda, Radiation field waveforms produced by lightning stepped leaders, *J. Geophys. Res.*, *80*, 2653–2657, 1975.

Le Vine, D. M., and R. Meneghini, Simulation of radiation from lightning return strokes: The effects of tortuosity, *Radio Sci.*, *13*, 801–809, 1978*a*.

Le Vine, D. M., and R. Meneghini, Electromagnetic fields radiated from a lightning return stroke: Application of an exact solution to Maxwell's equations, *J. Geophys. Res.*, *83*, 2377–2384, 1978*b*.

Le Vine, D. M., and R. Meneghini, A solution for the electromagnetic fields close to a lightning discharge, paper presented at the International Aerospace and Ground Conference on Lightning and Static Electricity (ICOLSE), Natl. Interagency Coord. Group of the Natl Atmos. Electr. Hazards Prot. Program, Fort Worth, Tex., June, 1983.

Lin, Y. T., M. A. Uman, and R. B. Standler, Lightning return stroke models, *J. Geophys. Res.*, *85*, 1571–1583, 1980.

Master, M. J., and M. A. Uman, Transient electric and magnetic fields associated with establishing a finite electrostatic dipole, *Am. J. Phys.*, *51*, 118–126, 1983.

McLain, D. K., and M. A. Uman, Exact expression and moment approximation for the electric field intensity of the lightning return stroke, *J. Geophys. Res.*, *76*, 2101–2105, 1971.

Meneghini, R., Application of the Lienard-Wiechert solution to a lightning return stroke model, *Radio Sci.*, *19*, 1485–1498, 1984.

Rubinstein, M., and M. A. Uman, On the radiation field turn-on associated with traveling current discontinuities in lightning, *J. Geophys. Res.*, *95*, 3711–3713, 1990.

Rubinstein, M., and M. A. Uman, Transient electric and magnetic fields associated with establishing a finite electrostatic dipole, revisited, *IEEE Trans. ElectroMagn. Compat.*, *EMC-33*, 312–320, 1991.

Thomson, E. M., Radiation field from an in-cloud lightning process with arbitrary orientation, paper presented at the 8th International Conference on Atmospheric Electricity, Natl. Sci. Res. Counc., Uppsala, Sweden, 1988.

Uman, M. A., and D. K. McLain, Magnetic field of lightning return stroke, *J. Geophys. Res.*, *74*, 6899–6910, 1969.

Uman, M. A., and D. K. McLain, Radiation field and current of the lightning stepped leader, *J. Geophys. Res.*, *75*, 1058–1066, 1970.

Uman, M. A., R. D. Brantley, Y. T. Lin, J. A. Tiller, E. P. Krider, and D. K.McLain, Correlated electric and magnetic fields from lightning return strokes, *J. Geophys. Res.*, *80*, 373–376, 1975*a*.

Uman, M. A., D. K. McLain, and E. P. Krider, The electromagnetic radiation from a finite antenna, *Am. J. Phys.*, *43*, 33–38, 1975*b*.

Weidman, C. D., and E. P. Krider, Submicrosecond rise times in lightning return stroke fields, *Geophys. Res. Lett.*, *7*, 955–958, 1980.

Weidman, C. D., and E. P. Krider, Correction to "The fine structure of lightning return stroke waveforms," *J. Geophys. Res.*, *87*, 7351, 1982.

Willett, J. C., V. P. Idone, R. E. Orville, C. Leteinturier, A. Eybert-Berard, L. Barret, and E. P. Krider, An experimental test of the "transmission-line model" of electromagnetic radiation from triggered lightning return strokes, *J. Geophys. Res.*, *93*, 3867–3878, 1988.

Willett, J. C., J. C. Bailey, V. P. Idone, A. Eybert-Berard, and L. Barret, Submicrosecond intercomparison of radiation fields and currents in triggered lightning return strokes based on the transmission-line model, *J. Geophys. Res.*, *94*, 13,275–13,286, 1989.

D. M. Le Vine, Microwave Sensors Branch, Goddard Space Flight Center, Mail Code 675, Greenbelt, MD 20771.

J. C. Willett, Geophysics Directorate, Phillips Laboratory, Hanscom Air Force Base, MA 01731.

(Received February 21, 1991;
revised November 5, 1991;
accepted November 5, 1991.)